

4-12-2004

Gas-Diffusion Process in a Tubular Cathode Substrate of an SOFC, Part I: Theoretical Analysis of Gas-Diffusion Process under Cylindrical Coordinate System

Kevin Huang

University of South Carolina - Columbia, huang46@cec.sc.edu

Follow this and additional works at: https://scholarcommons.sc.edu/emec_facpub

 Part of the [Mechanical Engineering Commons](#)

Publication Info

Published in *Journal of The Electrochemical Society*, Volume 151, Issue 5, 2004, pages A716-A719.

©Journal of The Electrochemical Society 2004, The Electrochemical Society.

© The Electrochemical Society, Inc. 2004. All rights reserved. Except as provided under U.S. copyright law, this work may not be reproduced, resold, distributed, or modified without the express permission of The Electrochemical Society (ECS). The archival version of this work was published in *Journal of The Electrochemical Society*].

Publisher's Version: <http://dx.doi.org/10.1149/1.1688338>

Huang, K. (2004). Gas-Diffusion Process in a Tubular Cathode Substrate of an SOFC, Part I: Theoretical Analysis of Gas-Diffusion Process under Cylindrical Coordinate System. *Journal of The Electrochemical Society*, 151 (5), A716 - A719. <http://dx.doi.org/10.1149/1.1688338>

This Article is brought to you by the Mechanical Engineering, Department of at Scholar Commons. It has been accepted for inclusion in Faculty Publications by an authorized administrator of Scholar Commons. For more information, please contact digres@mailbox.sc.edu.



Gas-Diffusion Process in a Tubular Cathode Substrate of an SOFC

I Theoretical Analysis of Gas-Diffusion Process under Cylindrical Coordinate System

Keqin Huang^{*,z}

Siemens Westinghouse Power Corporation, Pittsburgh, Pennsylvania 15235, USA

In this the first part of a two-part paper, the gas-diffusion process through a thick and porous tubular cathode substrate of a solid oxide fuel cell (SOFC) was theoretically analyzed using classic Fick's diffusion equation under the cylindrical coordinate system. The effects of current density, temperature, oxygen diffusivity or porosity, wall thickness, and bulk p_{O_2} on the concentration (or pore in this paper) polarization were calculated and are presented graphically. The results clearly show a greater impact on pore polarization by current density, oxygen diffusivity, wall thickness, and bulk p_{O_2} , but not by temperature. In addition, the limiting current density, which is a characteristic of a material, was also derived based on the solved cylindrical-coordinated diffusion equation.

© 2004 The Electrochemical Society. [DOI: 10.1149/1.1688338] All rights reserved.

Manuscript submitted August 4, 2003; revised manuscript received November 17, 2003. This was in part Paper 1868 presented at the Paris, France, Meeting of the Society, April 26-May 2, 2003. Available electronically April 12, 2004

The process of oxygen reduction taking place at the cathode of a solid oxide fuel cell (SOFC) has been an active subject for many years in the SOFC community. The significance of such a study is to help understand the underlying oxygen-reduction mechanism and develop catalytically active cathode materials for SOFCs, particularly at operating temperatures below 800°C. Generally speaking, there are two major types of electrochemical polarizations associated with the cathodic kinetics, namely, activation and concentration, which account for the principal voltage loss at the cathode during operation of an SOFC. The activation polarization is usually referred to as a series of physicochemical processes involving O_2 adsorption/dissociation, surface diffusion of adsorbed O species (such as O^-), ionization at triple-phase boundary (TPB) and ionic transfer across the cathode/electrolyte interface. Depending upon the magnitude of mixed electronic and oxide-ion conduction and thickness of the cathode,^{1,2} the oxygen transport in the cathode could also include (i) incorporation of adsorbed O species directly into bulk cathode, and (ii) the O^{2-} diffusion through the bulk cathode. Due to the nature of solid-state diffusion, these processes in principle have a greater temperature dependence (higher activation energy). In other words, the oxygen reduction kinetics becomes sluggish as the temperature decreases. On the other hand, concentration polarization resulting from the concentration gradient of reactive species across the thickness of the cathode most likely results from a limited gas-diffusion process. The gas diffusion through pores in the cathode at a given cell current, therefore, largely determines the magnitude of concentration (or pore) polarization. For planar and anode-supported SOFCs, the concentration polarization at the cathode is negligible compared to its counterpart, activation polarization, simply due to a much thinner cathode layer. However, this contribution could be significant for tubular, cathode-supported SOFCs. In fact, gas diffusion through a thick and porous cathode substrate has been proven to be one of performance-limiting factors for Siemens Westinghouse Power Corporation's (SWPCs) tubular SOFCs. Therefore, a comprehensive understanding of the gas-diffusion process and its resulting pore polarization in thick and porous cathode is beneficial and indispensable for enhancing power density.

Gas diffusion through pores in a solid is essentially a mass-transport process.³ Many experimental and modeling studies have been conducted in recent years to illustrate the effect of gas diffusion, primarily in the porous anode substrate, on the performance of

an SOFC.⁴⁻⁶ In general, the mass flux through a porous solid is diffusive in nature under a constant system pressure and may involve only ordinary molecular diffusion, Knudsen diffusion, and surface migration. The latter is negligible if no diffusing gases are adsorbed in a mobile layer. Depending on pore size and mean free path, the overall mass transport can be either dominated by molecular or Knudsen diffusion or both in some cases. Based on well-developed capillary theories that are established on a relatively simple pore structure, equations for predicting the concentration gradient across SWPCs thick porous cathode substrates and the resulting pore polarization have been developed at SWPC in the past few years. The calculations clearly show that Knudsen diffusion is negligible compared to molecular diffusion within a pore size $\sim 10 \mu\text{m}$ in the cathode substrate. Therefore, only molecular O_2 diffusion is considered in this paper.

In this the first part of a two-part paper, a thorough theoretical analysis of the gas-diffusion process occurring in a thick and porous tubular cathode substrate is reported. Due to the unique geometry, the cylindrical coordinate system is required to solve precisely Fick's diffusion equation in the $r - \theta - z$ plane. The concentration polarization (hereinafter, pore polarization), measured as overpotential, is calculated from the solved diffusion equation and presented as a function of current density, temperature, diffusivity or porosity, bulk p_{O_2} , and wall thickness of the tube. The limiting current density, which is a material characteristic of cathode substrate, is also derived and presented as a function of the diffusivity of the cathode.

Pore Diffusion under the Cylindrical Coordinate System

General diffusion equations.—For tubular fuel cells, the gas-diffusion should be considered to undergo in a long circular cylinder in which diffusion is everywhere radial. Additionally, oxygen diffusion through stagnant N_2 in air has to be considered because only oxygen is the reactive species at the cathode/electrolyte interface. Therefore, the conventional Fick's equation under the cylindrical coordinate system must be modified into the following form

$$Q(\text{mol/s}) = -D_{O_2}^{\text{eff}} A \frac{dC}{dr} + xQ \quad [1]$$

$$A(\text{cm}^2) = (2\pi - 2\theta)rL$$

$$C(\text{mol/cm}^3) = \frac{P}{RT}$$

$$x = \frac{P}{P_{\text{total}}}$$

* Electrochemical Society Active Member.

^z E-mail: keqin.huang@siemens.com

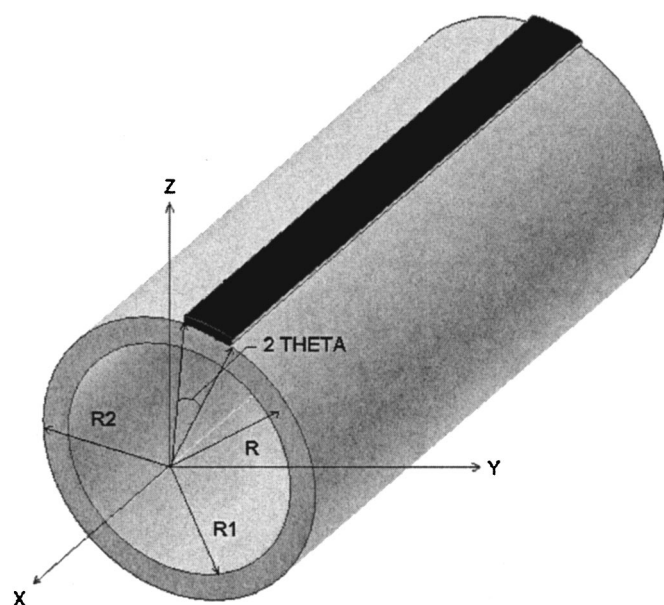


Figure 1. A geometrical schematic of O₂ pore diffusion under cylindrical coordinate system.

$$D_{\text{O}}^{\text{eff}}(T)(\text{cm}^2/\text{s}) = \frac{\varepsilon}{\tau} D_{\text{O}}(T) = \frac{\varepsilon}{\tau} D_{\text{O}}(293 \text{ K}) \left(\frac{T}{293} \right)^{1.5}$$

The meaning of each symbol is noted in the List of Symbols. A geometrical schematic illustrating the oxygen diffusion is shown in Fig. 1.

Rearrangement of Eq. 1 leads to the following equation

$$\frac{dr}{r} = -\frac{D_{\text{O}}^{\text{eff}}(2\pi - 2\theta)L}{RT} \frac{1}{Q} \frac{dp}{1 - \frac{p}{p_{\text{total}}}} \quad [2]$$

Integration of Eq. 2 from r_1 to r_2 (in cm) on the left side and the corresponding p_1 to p_2 (in atm) on the right side yields

$$\ln\left(\frac{r_2}{r_1}\right) = \frac{D_{\text{O}}^{\text{eff}}(2\pi - 2\theta)L}{RT} \frac{p_{\text{total}}}{Q} \ln\left(\frac{1 - \frac{p_2}{p_{\text{total}}}}{1 - \frac{p_1}{p_{\text{total}}}}\right) \quad [3]$$

At the cathode/electrolyte interface, according to Faraday's law, the passing current, I (A), has the following relationship with the incoming oxygen flux Q and current density J (A/cm²)

$$I = 4FQ = JL(2\pi - 2\theta)r_2 \quad [4]$$

Combining Eq. 3 and 4 gives the oxygen partial pressure p_2 at the interface

$$p_2 = p_{\text{total}} - (p_{\text{total}} - p_1) \exp\left[\left(\frac{RT r_2}{4FD_{\text{O}}^{\text{eff}} p_{\text{total}}}\right) J \ln\left(\frac{r_2}{r_1}\right)\right] \quad [5]$$

When the system pressure is at atmospheric conditions, Eq. 5 is simplified into

$$p_2 = 1 - (1 - p_1) \exp\left[\left(\frac{RT r_2}{4FD_{\text{O}}^{\text{eff}}}\right) J \ln\left(\frac{r_2}{r_1}\right)\right]$$

The resulting voltage loss or so-called pore polarization, η (V), across the substrate is then given by the Nernst equation

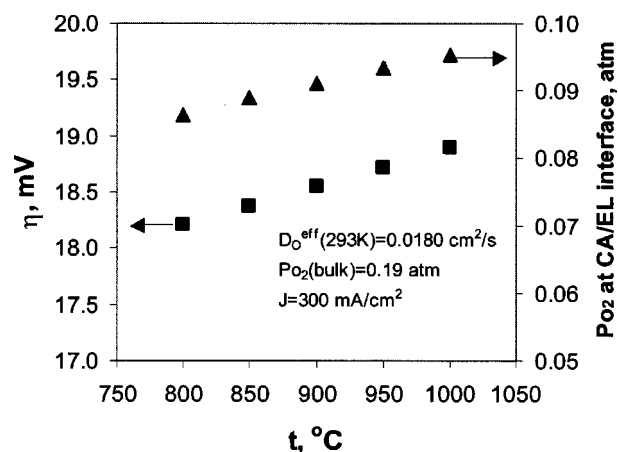


Figure 2. Pore polarization and interfacial p_{O_2} as a function temperature. CA/EL represents cathode/electrolyte.

$$\begin{aligned} \eta &= \frac{RT}{4F} \ln\left(\frac{p_1}{p_2}\right) \\ &= \frac{RT}{4F} \ln\left(\frac{p_1}{1 - (1 - p_1) \exp\left[\left(\frac{RT r_2}{4FD_{\text{O}}^{\text{eff}}}\right) J \ln\left(\frac{r_2}{r_1}\right)\right]}\right) \quad [6] \end{aligned}$$

It is clear that η is a function of temperature, bulk p_{O_2} in air, effective O₂ diffusivity, inside and outside radii of the cathode tube, and, of course, current density.

Limiting current density.—The limiting current density, J_L (A/cm²), is defined as the current density at which the interfacial oxygen partial pressure p_2 reaches zero, and is a characteristic of the material and a measure of material's resistance to concentration (pore) polarization. A higher J_L manifests a less polarized electrode. Set Eq. 5 to zero, the following equation can be obtained

$$J_L = -\frac{\ln(1 - p_1)}{\ln\left(\frac{r_2}{r_1}\right)} \times \frac{4FD_{\text{O}}^{\text{eff}}}{RT r_2} \quad [7]$$

It is clear that J_L depends on only the tube geometry, bulk p_{O_2} (p_1), and diffusivity for a given temperature. Among these variables, effective oxygen diffusivity or porosity has a profound impact on J_L .

Substituting Eq. 7 into Eq. 6, the pore polarization equation can be simplified into the following expression

$$\eta = \frac{RT}{4F} \ln\left(\frac{p_1}{1 - (1 - p_1)^{1 - J/J_L}}\right) \quad [8]$$

Application to the Cathode Substrate

In the following calculations, Eq. 6 is primarily used to demonstrate the effect of substrate porosity, cell current density, bulk p_{O_2} in air, wall thickness, and temperature. The tube inner and outer diameters were taken as 0.9 and 1.1 cm, respectively, for the following calculations except for the wall thickness discussion.

Effect of temperature.—The pore polarization and interfacial p_{O_2} (p_2) are plotted against temperature in Fig. 2, where $D_{\text{O}}^{\text{eff}}$ (293K) = 0.018 cm²/s, J = 300 mA/cm², and p_{O_2} = 0.19 atm (considering 16% oxygen utilization of air). It is evident that the magnitude of change in pore overpotential is relatively small as temperature varied from 800 to 1000°C. The observed slight in-

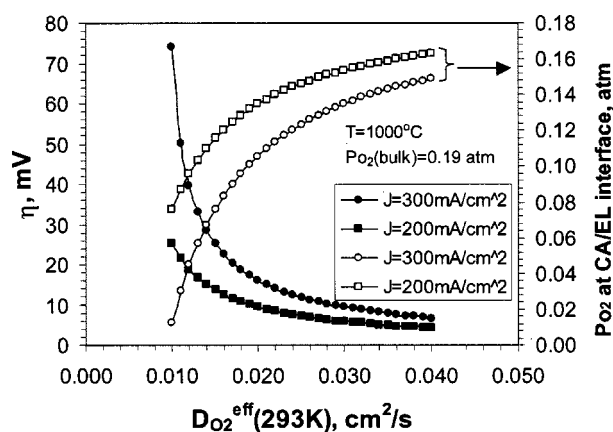


Figure 3. Pore polarization as a function of effective oxygen diffusivity of cathode substrate at 1000°C. CA/EL represents cathode/electrolyte.

crease of η on temperature is primarily due to the weak function of interfacial p_{O_2} on temperature, namely $p_{O_2} \propto T^{0.5}$ from Eq. 1 and 2. In the following discussion, therefore, only a representative temperature was used to illustrate other effects.

Effect of effective oxygen diffusivity (porosity).—The pore polarization and interfacial p_{O_2} at 1000°C and $p_{O_2}(\text{bulk}) = 0.19$ atm are plotted in Fig. 3 as a function of effective O_2 diffusivity at room temperature. For a typical value of $D_{O_2}^{eff}(293\text{ K}) = 0.018$ cm²/s, the voltage loss and interfacial p_{O_2} are shown to be approximately ~ 19 mV and ~ 0.09 atm, respectively, for cell current density of 300 mA/cm². (A typical value of $D_{O_2}^{eff}$ for SWPC's tubular substrates at room temperature.) The voltage loss appears to rise sharply at $D_{O_2}^{eff} < 0.015$ cm²/s. With decreasing the current density to 200 mA/cm², the voltage loss decreases and interfacial p_{O_2} increases as expected.

Pore polarization as a function of cell current density.—Similar to Fig. 3, the voltage loss and interfacial p_{O_2} are plotted in Fig. 4 against the cell current density at different levels of $D_{O_2}^{eff}$ under a condition of $T = 1000^\circ\text{C}$ and $p_{O_2}(\text{bulk}) = 0.19$ atm. It is again shown that the impact of $D_{O_2}^{eff}$ on the polarization is considerable. For $D_{O_2}^{eff} \leq 0.015$ cm²/s, the limiting current density is seen to approach the range of tubular fuel cell operating current density ≤ 500 mA/cm². This situation must be prohibited because the cathode sub-

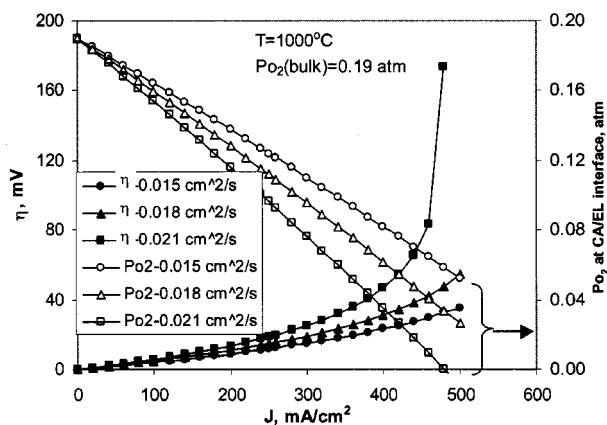


Figure 4. Pore polarization as a function of cell current density at 1000°C. CA/EL represents cathode/electrolyte.

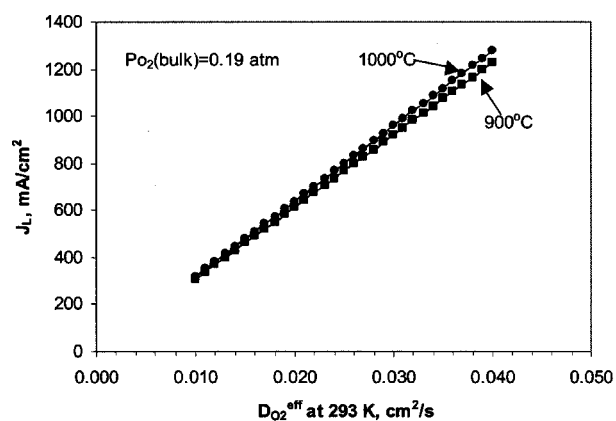


Figure 5. Limiting current density as a function of effective oxygen diffusivity.

strate can be heavily reduced due to an extremely low interfacial p_{O_2} at a current density close to J_L , causing destruction of the mechanical support.

Limiting current density.—According to Eq. 7, the limiting current density, one of material characteristics, was calculated and is shown in Fig. 5 as a function of $D_{O_2}^{eff}$ at 1000 and 900°C, respectively. It is no surprise to see that J_L increases with $D_{O_2}^{eff}$ because the polarization becomes lower and the interfacial p_{O_2} becomes higher at higher $D_{O_2}^{eff}$ as illustrated in Fig. 3 and 4. Again, the variation in temperature does not contribute a significant change in limiting current density.

Effect of bulk p_{O_2} in air.—The bulk p_{O_2} in air is solely determined by the oxygen utilization of air. Higher oxygen utilization or lower bulk p_{O_2} in air results in a lower interfacial p_{O_2} and therefore higher pore polarization. Figure 6 shows the calculated results of the pore polarization and interfacial p_{O_2} at 1000°C as a function of bulk p_{O_2} in air. The pore polarization is clearly shown to be strongly affected by a bulk p_{O_2} with a higher oxygen utilization. For example, by increasing oxygen utilization from 16 to 50% the pore polarization would be increased by five times (20 to 100 mV) at $J = 300$ mA/cm². As the oxygen utilization decreases the rate of

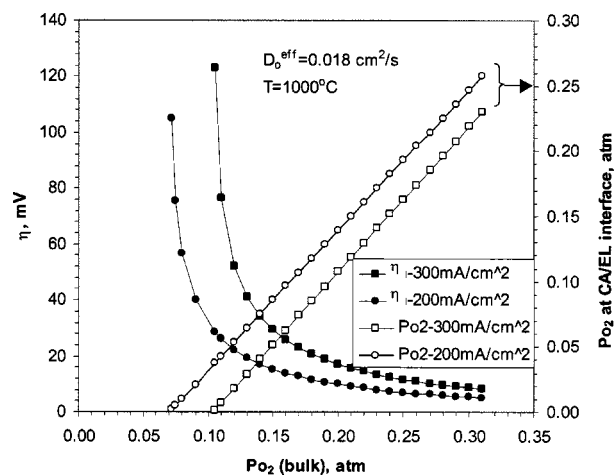


Figure 6. Pore polarization as a function of bulk p_{O_2} at 1000°C. CA/EL represents cathode/electrolyte.

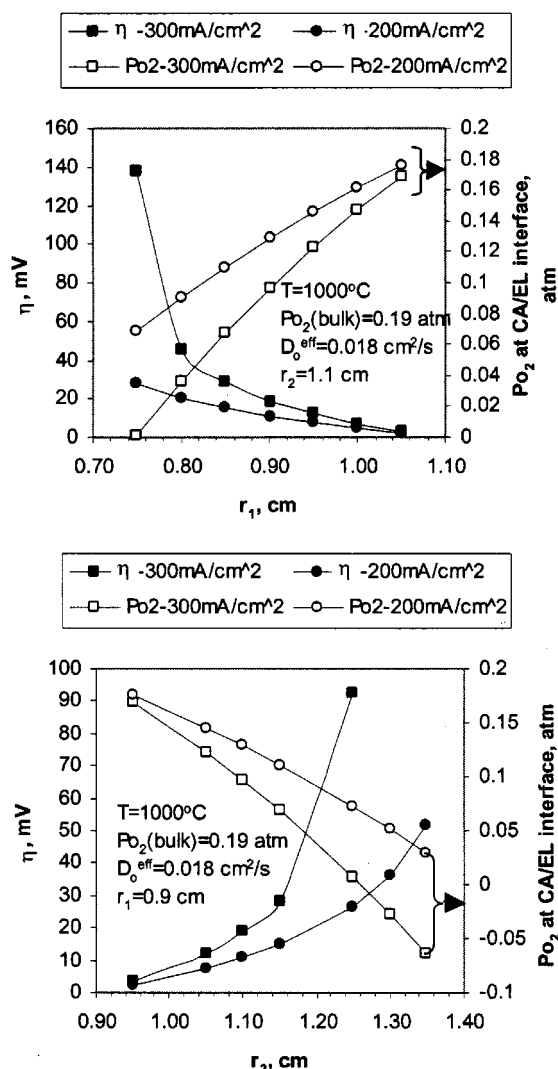


Figure 7. Pore polarization at 1000°C as a function of r_1 and r_2 . CA/EL represents cathode/electrolyte.

reduction in pore polarization tends to flatten out. Therefore, operating a cell at lower oxygen utilization is beneficial for cell performance in terms of concentration polarization.

Effect of wall thickness.—The sizes of r_1 and r_2 determine the wall thickness of the cathode tube. As the wall thickness is a variable affecting the pore polarization, the variations in r_1 and r_2 are expected to impact the pore polarization in the same manner. Figure 7 shows the calculated pore polarization at 1000°C as r_1 and r_2 change. A surprising finding was that the change in r_1 has a greater impact on polarization than r_2 at $J = 300 \text{ mA/cm}^2$. For example, increasing the wall thickness from 0.20 to 0.35 cm via decreasing r_1 from 0.90 to 0.75 cm at $r_2 = 1.10 \text{ cm}$, the pore polarization is increased by 626% ($19 \rightarrow 138 \text{ mV}$) at 300 mA/cm^2 . However, increasing the wall thickness by the same amount via increasing r_2 from 1.10 to 1.25 cm at $r_1 = 0.90 \text{ cm}$, the pore polarization is increased by only 384% at 300 mA/cm^2 . In neither case do r_1 and r_2 have appreciable influence on pore polarization at 200 mA/cm^2 . The calculations shown in Fig. 7 suggest that a larger r_1 would be beneficial for cell performance in terms of pore polarization.

Conclusions

The diffusion equations under the cylindrical coordinate system were developed for oxygen pore diffusion in SWPCs cathode substrate. It was explicitly shown that pore diffusion or polarization is a strong function of porosity (effective oxygen diffusivity) but a weak function of temperature in the range of 800 to 1000°C. As the porosity of the cathode substrate increases, the pore polarization decreases as a result of increased interfacial p_{O_2} . The limiting current density as one of the material characteristics evaluating cathode substrates was also derived from the solved diffusion equation. Higher porosity results in higher limiting current density, enabling the cathode substrate to be more resistant to concentration polarization.

On the other hand, the wall thickness and bulk p_{O_2} also have dramatic impacts on pore polarization. Higher oxygen utilization and smaller diameters of cathode tubes would adversely affect the cell performance in terms of pore polarization.

Acknowledgments

The author thanks the U.S. Department of Energy, National Energy Technology Laboratory, for financial support under Cooperative Agreement DE-FC26-97FT34139 and SECA program DE-FC26-02NT41247. Angela Bronson is also thanked for her assistance in manuscript preparation.

Siemens Westinghouse Power Corporation assisted in meeting the publication costs of this article.

List of Symbols

A	diffusion area, cm^2
C	oxygen concentration, mol/cm^3
D_O^{eff}	effective molecular oxygen diffusivity, cm^2/s
D_O	molecular oxygen diffusivity, cm^2/s
$D_O(293 \text{ K})$	molecular oxygen diffusivity at 293 K, cm^2/s
F	Faraday constant, 96,500 C/mole
I	cell current, A
J	cell current density, A/cm^2 or mA/cm^2
J_L	limiting current density, A/cm^2 or mA/cm^2
L	cell axial length, cm
P	oxygen partial pressure
p_1	bulk oxygen partial pressure in air, atm
p_2	interfacial oxygen partial pressure, atm
P_{total}	system pressure, atm
Q	oxygen flux, mol/s
r	radius of the cathode tube
r_1	inner radius of the cathode tube, cm
r_2	outer radius of the cathode tube, cm
R	gas constant, $82.057 \text{ cm}^3 \text{ atm/K mol}$
T	temperature, K
V	cell voltage, V
x	molar fraction of oxygen in air
z	the distance to $r - \theta$ plane

Greek

ε	porosity of the cathode substrate
η^{pore}	pore polarization, V or mV
θ	radian corresponding to half of the interconnection width, $\text{degree} \times \pi/180$
τ	tortuosity of the cathode substrate

References

- H. Fukunaga, M. Ihara, K. Sakaki, and K. Yamada, *Solid State Ionics*, **86-88**, 1179 (1996).
- M. Koyama, C.-J. Wen, T. Masuyama, J. Otomo, H. Fukunaga, K. Yamada, K. Eguchi, and H. Takahashi, *J. Electrochem. Soc.*, **148**, A795 (2001).
- G. R. Youngquist, in *Flow Through Porous Media*, p. 57, American Chemical Society Publications, Washington, DC (1970).
- R. E. Williford, L. A. Chick, G. D. Maupin, S. P. Simmer, and J. W. Stevenson, *J. Electrochem. Soc.*, **150**, A1067 (2003).
- J. W. Kim, A. V. Virkar, K. Z. Fung, K. Mehta, and S. C. Singhal, *J. Electrochem. Soc.*, **146**, 69 (1999).
- P. Costamagna and K. Honegger, *J. Electrochem. Soc.*, **145**, 3995 (1998).